Enhanced cohesion promotes chromosome stability and limits acquired drug resistance in non small cell lung cancer

Nicole M Hermance[1], Elizabeth A Crowley[1], Conor P Herlihy[1], Amity L Manning[1*]

[1] Department of Biology and Biotechnology, Worcester Polytechnic Institute, Worcester, MA, 01609 USA

[*]corresponding author:
Amity L Manning
Email: almanning@wpi.edu
tel: 508-831-4961

Abstract

Chromosome instability, or CIN, defined as a high frequency of whole chromosome gains and losses, is prevalent in many solid tumors. CIN has been shown to promote intra-tumor heterogeneity and correspond with tumor aggressiveness, drug resistance and tumor relapse. However, whether CIN promotes the acquisition of genomic changes responsible for drug resistance remain unclear. Here we assess the role of CIN in the acquisition of drug resistance in non small cell lung cancer. We show that impairment of centromeric cohesion underlies the generation of whole chromosome segregation errors and CIN in non small cell lung cancer cells. Further, we demonstrate that centromere-specific enhancement of chromosome cohesion strongly suppresses CIN and reduces intra-tumor heterogeneity. We demonstrate that suppression of CIN has no impact on NSCLC cell proliferation *in vitro* nor in tumor initiation in mouse xenograft models. However, suppression of CIN alters the timing and molecular mechanism that drive acquired drug resistance. These findings suggest mechanisms to suppress CIN may serve as effective co-therapies to limit tumor evolution and sustain drug response.

Introduction

Whole chromosome instability (CIN), defined as a persistently elevated rate of chromosome mis-segregation, is generated by underlying defects in mitosis[1, 2]. The aneuploid chromosome content that results from mitotic segregation errors promotes intra-tumor heterogeneity and is a driving force in cancer that contributes to tumor evolution and drug resistance [1-5]. Chromosome segregation is exquisitely sensitive to the regulation of dynamic microtubule attachments and defects that either increase or decrease the stability of microtubule attachments can corrupt mitotic fidelity and contribute to CIN [6, 7]. Conversely, perturbations that reduce CIN are proposed to limit acquired drug resistance and may hold therapeutic potential.

Aurora B kinase is a master regulator of kinetochore-microtubule dynamics during mitosis. Its overexpression is common in many cancer contexts and recent analyses of over 10,000 cancer genomes from the Cancer Genome Atlas shows that, across cancer subtypes, Aurora B expression corresponds with degree of aneuploidy [8]. Increased expression of Aurora B also correlates with poor patient prognosis in a variety of cancer contexts [9]. Aurora B is a component of the Chromosome Passenger Complex (CPC). The CPC localizes to the centromere where Aurora B kinase activity regulates localization and activity of numerous kinetochore components involved in binding and stabilizing kinetochore microtubule attachments, thereby promoting satisfaction of the spindle assembly checkpoint and regulating chromosome segregation [10]. Consistent with this function, both decreased and increased Aurora B centromere activity results in chromosome segregation errors [11-16].

The cohesin complex is loaded onto chromatin concurrent with replication and functions to hold replicated sister chromatids together, termed cohesion, prior to anaphase onset. This role for cohesin is important to ensure proper attachment of replicated sisters such that each chromatid

attaches to microtubules emanating from opposite poles of the mitotic spindle. Here we demonstrate that Aurora B is negatively regulated by cohesin such that global or centromere-specific enhancement of cohesion reduces centromere-localized Aurora B. In a panel of non small cell lung cancer (NSCLC) cell lines, where Aurora B is overexpressed and rates of chromosome segregation are high, enhancement of centromere cohesion is sufficient to reduce Aurora B at centromeres, minimize genomic heterogeneity and limit whole chromosome amplifications, without altering cell proliferation. We additionally find that suppression of CIN limits acquired drug resistance both *in vitro* and *in vivo*, and that sustained CIN is rate limiting for tumor relapse.

Materials and Methods

Cell culture, protein expression and depletion

PC9, H1299, and A549 (ATCC) cells were grown in RPMI1640 (Gibco) medium supplemented with 10% fetal bovine serum (Sigma) and 1% penicillin/streptomycin (Gibco). hTERT-RPE-1 (RPE) (ATCC) cells were grown in Dulbecco's Modified Eagles Medium (DMEM) supplemented with 10% fetal bovine serum (Sigma) and 1% penicillin/streptomycin (Gibco). All cells were cultured at 37°C and 5% CO2. High resolution immunofluorescence imaging with DNA stain (DAPI) is used to monitor and confirm cell lines are free of *Mycoplasma* contamination. For short term knock down of targets, 50nM pool siRNAs (non-targeted pool or a pool of 4 siRNAs to Wapl (Dharmacon-ON-TARGETplus Human Wapl siRNA-SMARTpool) were transfected using RNAiMax (ThermoFisher) transfection reagent according to the manufacturer's instruction, or alternatively infected with a lentiviral construct containing an shRNA hairpin for constitutive (pLK0.1-Puro) or doxycycline inducible (tet-pLK0-Puro) depletion. Stable hairpin-expressing clones were selected with Puromycin for 7-10 days. Induced depletion was achieved by the addition of 2μg/ml doxycycline for a minimum of 48 hours. Expression of a centromere

targeted GFP-sororin (CEN-Sororin-GFP) was achieved by sub-cloning human Sororin cDNA into the CENP-B DBD INCENP GFP vector (45237, Addgene) using Nhe1/BamH1. Expression vectors were transfected using Lipofectamine 3000 (Invitrogen) according to manufacturer's instructions and stable integrations selected with G418 for 7-10 days.

For quantification of mRNA expression levels for Wapl, Aurora B, EGFR, Slug, Vimentin and MET expression in cell lines, drug tolerant clones, or tumors following Gefitinib treatment with or without Wapl depletion, RNA was extracted from cell lines or frozen tumors using Trizol reagent (Invitrogen) according to the manufacturer's instructions. Complementary DNA was synthesized from 2μg of total RNA using Superscript First-Strand Synthesis System (Invitrogen) and random hex primers. Gene expression was determined by using the ΔΔ cycle threshold method normalized to *GAPDH.* Primer sequences used for qRT-PCR can be found in Supplemental Table 1. Samples were run as technical duplicates and the experiment performed in 3 biological replicates. Data presented represents average and standard deviation between biological replicates. A students' 2-tailed t-test was used to determine statistical significance.

To assess protein levels, whole cell extracts were prepared using 2x Laemmli buffer (Sigma Aldrich) with β–Mercaptoethanol. Protein concentrations were normalized to total cell number and samples run on an SDS-PAGE gel. Proteins were transferred to PVDF membrane (Millipore) and membranes blocked in 1xTBST supplemented with 5% milk powder. Antibodies were diluted in 1xTBST/5% milk (phospho EGFR (Cell Signaling), total EGFR (Cell Signaling), total MET (Cell Signaling), total ERK (Cell Signaling), WAPL (Bethyl), Aurora B (BD Biosciences), Histone H3 (Abcam), and alpha-tubulin (Santa Cruz)) or 1xTBST/5%BSA (phospho MET (Cell Signaling), phospho ERK (Cell Signaling)) and incubated at 4° overnight. Membranes were washed in 1xTBST and incubated 1h in corresponding secondary antibody

(rabbit, mouse: GE Healthcare), washed in 1xTBST buffer and developed using ProSignal Pico (Prometheus).

Immunofluorescence and Fluorescence *in situ* hybridization

Cultured cells or single cell suspensions derived from tumors were grown on coverslips fixed, and stained for Aurora B (BD Biosciences), ACA (Antibodies Inc), tubulin (Santa Cruz), and GFP (Abcam) as previously described [17]. Fluorescence *in situ* hybridization with centromeric probes and quantification of numerical heterogeneity was performed as previously described in [18] using alpha satellite-specific probes for chromosomes 2,6,7,8 and 10 (Cytocell). For FISH from tumors, single cell suspensions were made by gently grinding tumors between two glass slides and culturing with continued drug treatment for 3-5 days. Cells were then collected and processed as above. Clonal Numerical Heterogeneity (NH) of a population was determined by scoring >300 cells per clone/tumor for copy number for chromosome probe (assessed in pairs) to determine the modal copy number, and the fraction of cells deviating from that number (i.e. the numerical heterogeneity). A given copy number with greater than 20% prevalence in a population was considered too be stable subclone and not included in the numerical heterogeneity score. Data is represented for individual chromosomes, or alternatively, as average NH across all chromosomes for a given sample. A students' 2-tailed t-test was used to determine statistical significance.

Images were captured using a Zyla sCMOS camera mounted on a Nikon Ti-E microscope, with a 60X Plan Apo oil immersion objective and capturing 0.3 μm z-stacks. To assess centromeric Aurora B levels, NIS-elements Advanced Research software was used to perform line scans in a single focal plane through individual ACA-stained kinetochore pairs where interkinetochore distance is represented by the distance between ACA peaks, and the area under the curve in the Aurora B-stained channel indicates centromere/kinetochore-localized Aurora B. For

interkinetochore distances and Aurora B localization a minimum of 3 kinetochore pairs per 30 cells, per condition (90 kinetochore pairs/condition) were measured in each of 3 biological replicates. Anaphase defects were assessed in a minimum of 30 cells per condition, in each of 3 biological replicates. Data presented represents average and standard deviation between biological replicates. A students' 2-tailed t-test was used to determine statistical significance. For figure generation, images were prepared using NIS Elements deconvolution software and represented as projections of 5 central plains. Insets represent a single focal plane.

Growth and survival analyses

Proliferation rates of PC9 clones stably expressing a doxycycline inducible construct to target Wapl for depletion were plated in 6 well dishes at $5x10^4$ cells per well in the presence or absence of 2 μg/ml doxycycline. Cells were collected and counted for 5 consecutive days using a Luna II Automated Cell Counter. Anchorage-free proliferation assays were performed in PC9 cells with or without constitutive shRNA-depletion of Wapl. 4×10^4 cells were mixed with 0.4% agarose in growth medium (RPMI 1640 supplemented with 10% FBS, 1% penicillin/streptomycin), plated in a 6 well dish containing a solidified layer of 0.5% agarose in growth medium and placed at 4° for 15 minutes to allow solidification. Cells were fed once a week with 2% agarose in growth medium. At 4 weeks colonies were imaged and counted. Data presented represents average and standard deviation between three biological replicates. A students' 2-tailed t-test was used to determine statistical significance.

To determine cell viability PC9 cells carrying an inducible shRNA construct to deplete Wapl were plated in 96 well dishes at 3000 cells per well and treated with or without 2μg/ml doxycycline (Sigma) in addition to treatment with either DMSO or 0.2μM, 0.4μM, 0.6μM, 0.8μM, 1.0μM or 1.2μM Gefitinib (Selleckchem). Cells were cultured for 3 days and viability was

assessed using Presto Blue (Invitrogen). Absorbance values were normalized to the untreated control. Each condition was plated in technical triplicate and the entire assay was performed in 3 biological replicates. Data is represented as average and standard deviation between biological replicates. A students' 2-tailed t-test was used to determine statistical significance. For *in vitro* drug tolerance assays $1x10^4$ PC9 shWapl cells were plated in a 10 cm dish with or without 2μg/ml doxycycline. Cells were then treated with 1μM Gefitinib (Selleckchem). Growth medium containing drug was replaced twice per week. At 2 and 4 weeks cells were washed in 1xPBS and fixed and stained with 0.5% (w/v) crystal violet (Gibco) in 25% methanol (v/v) (Sigma) for 30 min, rinsed 3 times with water, dried and colonies were counted. Data presented represents average and standard deviation between three biological replicates. A students' 2-tailed t-test was used to determine statistical significance.

***In vivo* tumor growth and relapse assays**

Eight-week old male and female Crl:NU-*Foxn1*^{nu} mice (stock #088) were purchased from Charles River Laboratory and maintained in a pathogen-free facility. All animal experiments were performed in accordance with institutional regulations after protocol review and approval by Worcester Polytechnic Institute's Institutional Animal Care and Use Committee.

For *in vivo* growth assays, three cohorts of 5 mice each were injected subcutaneously in the flank with $5x10^6$ PC9 cells. 2 cohorts received PC9 cells expressing a tetracycline-inducible shWapl expression construct. One of these two cohorts was administered 2 μg/ml doxycycline in the drinking water. All three cohorts were monitored daily and tumor size measured 3x/week. Mice were humanly sacrificed, and tumor tissue collected when tumor volume reached $300mm^3$. For tumor relapse studies, tumor xenografts were generated as described above in 40 mice. Xenograft tumor formation was observed in 38 mice. Once tumors reached a size of $300mm^3$

mice were randomized equally into a minus or plus doxycycline group. All mice were given 50mg/kg Gefitinib (Selleckchem) by oral gavage following a 5 day on and 2 day off cycle. Mice were monitored daily and tumor size measured 3x/week to monitor tumor regression and relapse. Once relapsed tumors reached a size of 300mm^3 mice were humanly sacrificed, tumors harvested and frozen or cultured for subsequent experimental analysis.

EGFR sequencing

Total RNA was isolated from primary mouse tumors using Trizol (Invitrogen). cDNA was transcribed with Superscript First-Strand Synthesis System (Invitrogen) and used as template for subsequent PCR based studies. EGFR was amplified by PCR and products were cloned into a TOPO TA cloning vector (Invitrogen), transformed into bacteria and the inserts from individual clones sequenced. Primers are listed in Supplemental Table 1.

Results

Chromosome segregation errors in NSCLC cells are sensitive to cohesion regulation

Work from our group and others has demonstrated that compromised chromosome cohesion promotes mitotic segregation errors. [19, 20]. To test whether defects in chromosome cohesion may similarly underlie segregation errors and CIN in NSCLC cells, we first identified a panel of NSCLC cell lines that exhibit mitotic defects and chromosome copy number heterogeneity consistent with CIN (A549, H1299, and PC9; [18], Figure 1 and Supplemental Figure 1A & B). Enhancement of chromosome cohesion was achieved using si- and sh-RNA approaches to deplete Wapl, a well-characterized negative regulator of the cohesin complex [21] (Figure 1A & Figure 2). Wapl is associated with the cohesin complex and regulates its dynamic association with chromatin throughout the cell cycle [22]. Wapl depletion blocks cohesin complex dissociation from chromosomes during early mitosis. We used immunofluorescence imaging of metaphase cells to identify and measure inter-kinetochore distances as a readout of functional

centromere cohesion. This demonstrated that Wapl knockdown (Wapl KD) enhanced cohesion, as evidenced by a statistical reduction in interkinetochore distance (Figure 1B & C). We then assessed mitotic fidelity in these cells. We demonstrate that enhancement of chromosome cohesion, via Wapl depletion, is sufficient to reduce the incidence of lagging chromosomes during anaphase (Figure 1D & E).

Frequent high rates of whole chromosome segregation errors during mitosis contribute to genomic heterogeneity within a cell population that can be assessed using FISH-based approaches to measure population-level numerical heterogeneity (NH) for individual chromosomes. To assess if enhanced cohesion and reduction of anaphase defects is sufficient to suppress CIN, PC9 cells were engineered to constitutively express one of two different shRNA hairpin constructs designed to target Wapl mRNA for depletion. Single cell clones were derived from parental and Wapl-deficient PC9 cells and analyzed for NH. Individual clones derived from PC9 cells expressing an empty PLK0.1 vector exhibit NH values of 18-31% for chromosome 6, and up to 20-40% for chromosome 2. NH for both chromosomes was reduced ~2-3-fold in Wapl-deficient PC9 cell clones (chromosome 6: 3-12%, chromosome 2: 5-24%) (Figure 1F), indicating that enhanced cohesion is sufficient to suppress CIN.

Centromere localization of the mitotic Aurora B kinase is limited by cohesion.

Aurora B kinase, an important regulator of mitotic chromosome segregation and the mitotic spindle assembly checkpoint, is commonly overexpressed in non small cell lung cancer where CIN is also prevalent [23-25]. Our data confirm that global Aurora B protein levels are dramatically higher in our panel of NSCLC cell lines than in a similarly proliferative epithelial cell line (RPE) (Figure 2A). To test the hypothesis that Wapl depletion suppresses CIN by mitigating high Aurora B levels or activity, western blot and immunofluorescence assays were employed to assess global and centromere-specific Aurora B levels in the presence and absence of Wapl.

We find that depletion of Wapl does not alter high Aurora B levels in these cell lines (Figure 2A), but instead perturbs Aurora B localization such that centromere-localized Aurora B levels in all three NSCLC lines is reduced by ~50% when Wapl is depleted (Figure 2B & C). Together, these data support a model whereby increased Aurora B activity underlies CIN in NSCLC cells.

In addition to its role in mitotic chromosome cohesion and centromere regulation, the cohesin complex also functions in gene regulation and nuclear architecture throughout the cell cycle. Therefore, to specifically assess the role of centromere cohesion in regulating CIN in NSCLC, we employed a centromere-targeted Sororin fusion protein. Sororin is a positive regulator of cohesion and its targeted localization to centromeres has been demonstrated to enhance cohesin complex enrichment specifically at the centromere [26, 27]. In these experiments, GFP-tagged Sororin was targeted to centromeres through a fusion to the DNA binding domain of CENtromere Protein B (CENPB). CENPB binds specifically to a DNA sequence found at and near centromeres [28-30] and the Sororin fusion protein (CEN-Sororin-GFP) is efficiently targeted to mitotic centromeres in the H1299 cell line (Figure 2D). Consistent with its role in enhancing centromere cohesion, expression of CEN-Sororin-GFP reduces inter-kinetochore distance (Figure 2D & E). Similar to Wapl depletion, CEN-Sororin-GFP expression also results in a decrease in centromere Aurora B levels (Figure 2D & F). Together these data suggest Aurora B localization at centromeres is not dependent on Wapl activity *per se* but is instead generally sensitive to enhanced centromere cohesion.

Suppression of CIN limits drug tolerance in NSCLC cells.

Activating mutations within the EGFR gene that drive tumor cell proliferation are present in nearly a quarter of all NSCLCs [31]. Patients with such mutations are commonly treated with EGFR tyrosine kinase inhibitors (TKIs) [32]. However, the majority of patients treated with EGFR TKIs ultimately develop resistance with nearly 60% of resistant or relapsed tumors

exhibiting resistance-conferring mutations in the EGFR gene, making this the most frequent mechanism of EGFR TKI resistance [33]. PC9 cells exhibit an activating deletion in exon 19 of EGFR that drives cell proliferation and renders them sensitive to EGFR TKIs [34]. Like tumors in patients, these cells commonly acquire resistance to EGFR TKIs via acquisition of a secondary Threonine to Methionine mutation in EGFR (T790M) [33]. While CIN in NSCLC, and other cancer contexts, has been correlated with acquired drug resistance [5, 23, 35], the impact of CIN on mutation-based mechanisms of acquired drug resistance remain unclear.

Drug response is sensitive to cell proliferation rates and the impact of aneuploidies that result from CIN have alternatively been demonstrated to promote tumor cell growth or to reduce proliferative capabilities [36, 37]. Therefore, we first assessed proliferative capacity of PC9 cells with and without constitutive CIN/Wapl depletion (Mock and Wapl KD, respectively). First, doubling times were measured for clonal PC9 cells engineered to express a tetracycline-regulated shWapl hairpin with and without induction of hairpin expression. Importantly, in all clones tested, proliferation rates with or without Wapl depletion, when grown in the absence of TKI treatment, were comparable (Figure 3A). Similarly, anchorage independent colony formation assays of growth in soft agar revealed similar colony number and size, irrespective of Wapl/CIN status (Figure 3B & C), indicating that suppression of CIN alone does not alter drug naïve PC9 cell growth.

Next we assessed the response of cells, with and without Wapl depletion, to the EGFR TKI Gefitinib. EGFR activity results in phosphorylation of EGFR and downstream targets (such as ERK) and promotes cell proliferation. Western blot and viability assays indicate that PC9 cells with either mock or induced Wapl depletion are initially similarly responsive to Gefitinib: both populations show dramatic reduction of EGFR-dependent phosphorylation (phospho EGFR: Tyr1068 & phospho ERK: Tyr 202/Tyr 204) and similar dose-dependent reduction in viability

following short term exposure (Figure 3D & E). Nevertheless, following 4 weeks of continuous treatment with a sub-lethal dose of Gefitinib drug-tolerant cells slowly form colonies that can be detected with crystal violet stain (Figure 3F). In contrast, following long-term exposure to Gefitinib, Wapl depleted PC9 cells exhibit a dramatic reduction in the number and size of drug tolerant colonies that arise while under TKI treatment (Figure 3F & G). These data suggest that CIN promotes acquisition of drug tolerance to permit continued proliferation.

Chromosome Instability informs mechanism of TKI drug resistance.

To better understand the relationship between CIN-dependent genomic changes that may promote or permit resistance to drug therapy we characterized four drug-tolerant clones from each population exposed to long-term Gefitinib treatment. Clones were selected and expanded under culture conditions that maintained 1μM Gefitinib and mock or induced Wapl depletion, as appropriate. Importantly, in both Wapl-depleted and Wapl-proficient contexts, drug tolerant PC9 cells that persist following long term exposure to Gefitinib continue to exhibit features consistent with Wapl status: single colonies derived from Mock-depleted cells have frequent anaphase defects and a high measure of NH while Wapl-depleted cells have reduced anaphase defects and less numerical heterogeneity (Figure 4A-C, Supplemental Figure 2A & B).

Cells that acquire tolerance or resistance to TKI activity do so by restoring or bypassing EGFR kinase function to activate downstream pathway components and promote proliferation [33]. Although the emergence of drug tolerant clones is decreased significantly by Wapl depletion, molecular characterization of EGFR pathway function indicates that drug tolerant clones that do arise from both Mock- and Wapl-depleted populations similarly exhibit phosphorylation of ERK, a downstream target in the EGFR pathway (Figure 4D). In contrast, Wapl-depleted PC9 clones, but not Mock-depleted PC9 clones, additionally exhibit EGFR auto phosphorylation (Figure 4D). This phosphorylation is dependent on EGFR kinase activity and suggests drug-tolerant clones

that lack CIN (Wapl KD) primarily arise through the acquisition of resistance-conferring mutations that impair TKI binding, while clones that sustain CIN (Mock) likely exploit other mechanisms of drug tolerance [31-33, 38].

Alternative pathways reported to promote TKI resistance in NSCLC include amplification of EGFR, amplification of the receptor tyrosine kinase MET [38], and/or activation of epithelial to mesenchymal transition (EMT) [39-41]. To understand if these alternative pathways could explain tolerance of Mock- depleted PC9 clones to Gefitinib treatment, we first assessed copy number of chromosome 7, on which both EGFR and MET genes are located. Drug naïve PC9 cells have a modal copy number of four for chromosome 7, as do drug tolerant Wapl-depleted clones. In contrast, nearly 60% of drug tolerant Mock-depleted cells have >8 copies of chromosome 7 (modal copy number in parental PC9 cells is 4; Supplemental Figures 1A, 2A & 2B). Nevertheless, protein and activation (phosphorylation) levels of EGFR and MET kinase show no increase over that seen in drug naïve PC9 cells (Figure 3D and Figure 4D & E) to suggest either of these as a mechanism for resistance. We next looked at expression of key EMT transcription factor SLUG and found it to be upregulated 2-fold in 3 out of 4 Mock-depleted clones, but not in any of the Wapl-depleted clones (Figure 4E). The gene that encodes for SLUG, SNAI2, is located on chromosome 8p, adjacent to the centromere. In support of a model whereby CIN influences the mechanism of TKI resistance, single cell analysis of chromosome 8 copy number indicates that the same 3 Mock-depleted clones with increased SLUG expression also exhibit amplification of chromosome 8 (Figure 4C and Supplemental Figure 2A). Consistent with SNAI2 amplification and increased Slug expression, Vimentin, a widely used marker of EMT and a Slug target gene is also increased 2 to12-fold in Mock-depleted clones (Figure 4E). Together these data suggest that CIN influences the mechanism of acquired drug resistance. Without CIN, mutation-driven mechanisms of drug resistance dominate, but the acquisition of such mutations are slow, particularly in drug treated populations with limited proliferation and as

a result drug resistant colonies are slow to emerge. Through whole chromosome gains and losses hundreds to thousands of genes may become mis-regulated in a single cell division. In this way CIN has the capacity to promote cellular changes that are selected for and that contribute to drug tolerance.

Wapl depletion is sufficient to suppress CIN *in vivo*

To assess how cohesion-dependent suppression of CIN impacts tumor initiation and growth *in vivo*, PC9 cells with or without a tetracycline-inducible shWapl construct were injected subcutaneously into the flanks of nude mice to generate 3 cohorts: one with parental PC9 cells, and two with PC9 cells that harbor the inducible shWapl construct (Figure 5A). One cohort of PC9 shWapl mice then received doxycycline in the drinking water to induce expression of the Wapl-targeting hairpin throughout the duration of tumor initiation and growth. The cohort injected with the PC9 parental cell line similarly received doxycycline in the water as a negative control. Tumor initiation was comparable in all three cohorts of mice, as was rate of tumor growth (Figure 5B, Supplemental Figure 3A). To confirm the efficiency of Wapl depletion and the suppression of CIN in response to doxycycline treatment *in vivo*, tumors from mice in each cohort were excised when they reached 300cm^3 and subjected to analysis. Quantitative PCR analyses confirm that depletion of Wapl mRNA and protein levels were achieved and sustained during tumor initiation in response to doxycycline (Figure 5C). Consistent with *in vitro* assays, cells derived from Wapl-deficient tumors exhibit fewer anaphase defects (Figure 5D) and less intra-tumor chromosome numerical heterogeneity (Figure 5E). Together these data indicate that suppression of CIN in NSCLC cells is not in itself sufficient to limit tumor initiation and growth *in vivo*.

CIN is a driver of drug resistance in *vivo*

To test the role of CIN in tumor relapse, the xenograft model described above was used to establish mice that harbored inducible PC9 shWapl tumors. Once tumors reached a volume of 300mm^3, mice were put on a 5 days on, 2days off (5+2) regimen of 50 mg/kg Gefitinib treatment and randomly assigned to two cohorts- one received doxycycline in the drinking water to induce Wapl depletion concurrent with Gefitinib treatment, the other did not (Figure 6A). Both cohorts of mice exhibited similar initial response to Gefitinib, with all tumors exhibiting >50% recession within 2 weeks. In the 100 days following initial tumor recession mice were sustained on a 5+2 drug regimen. During this time 37% (7/19) of Mock-depleted tumors and 21% (4/19) of Wapl depleted tumors relapsed. Relapse of Wapl depleted tumors was delayed by nearly 3 weeks compared to those without induced Wapl depletion (66 days vs 46 days for Mock depleted tumors) (Figure 6B & C, Supplemental Figure 3C). A similar frequency of the TKI resistance-conferring EGFR T790M mutation was detected in relapsed tumors from both cohorts (Figure 6D & E). Interestingly, anaphase defects were similarly prevalent in all relapsed tumors, regardless of cohort, indicating a selective pressure to maintain CIN during acquisition of drug resistance (Supplemental Figure 3B). Consistent with this, all residual/non-relapsed tumors analyzed from the Wapl depleted cohort sustained Wapl depletion while those that relapsed expressed Wapl at levels comparable to the Mock-depleted cohort (Figure 6F). These data support a model whereby re-establishment of Wapl expression/CIN, or expansion of clones that fail to silence Wapl/sustain CIN, is limiting for acquired drug resistance and tumor relapse (Figure 7).

Discussion

Clonal mutations that enable resistance to targeted or chemotherapeutic approaches pose a clinical challenge and remain a major cause of death in many cancer types [42]. Clinically and experimentally, the degree of intra-tumor genomic heterogeneity, and underlying defects in mitotic cell division have been functionally linked to tumor evolution, drug resistance, and

metastasis [3, 4, 43, 44]. In the context of NSCLC, identification of driver mutations in EGFR and the initial clinical success of TKI treatment has been hampered by rapid and prevalent acquisition of drug resistance [31]. Here, we present mechanistic evidence that, in the context of NSCLC, CIN may arise from mis-regulation of cohesin-sensitive Aurora B kinase activity at centromeres and that subsequent chromosome amplifications contribute to a high incidence of acquired resistance to targeted therapy. The reduction in emergence of drug tolerant clones following experimental suppression of CIN demonstrate that whole chromosome copy number changes create a favorable environment for continued proliferation while resistance-conferring EGFR mutations are attained. Consistent with this, we find that a selective pressure exists *in vivo* to maintain or re-establish CIN to facilitate robust acquisition of drug resistance and tumor relapse (Figures 6 & 7).

Whole chromosome segregation errors enable tumor evolution and drug resistance

Our analysis examined isogenic PC9 cells that primarily differ, at least initially, in their CIN status. Our results indicate that CIN contributes to drug resistance by allowing for the generation of whole chromosome amplifications that harbor key drug tolerance genes (like EGFR, MET, and SNAI2/SLUG) and promote continued proliferation in the presence of TKI. In the absence of an increased mutation rate, this continued proliferation is key to enable the acquisition of replication-dependent mutations that confer robust drug resistance and tumor relapse. Such adaptive mutability may be particularly relevant to the mis-segregation and subsequent selection for amplification of chromosome 7, which contains both MET and EGFR genes. Increased EGFR gene copy number both promotes proliferation [33] and, by virtue of having more EGFR gene templates for replication-acquired mutation, increases the apparent mutability of individual cells [45]. These findings are consistent with pervious studies showing selective pressure for cancer cells to sustain CIN [46, 47].

High mutation rates may preclude the need for CIN in acquired drug resistance.

In the absence of CIN, resistance is limited to the clonal amplification of cells with pre-existing amplifications or mutations, and those that acquire chromosome amplifications through rare segregation errors. An increase in mutation rate may negate the need for CIN by increasing the frequency at which resistance-conferring mutations are generated in each cell cycle. Consistent with this view, high mutation rates and CIN have been found to be mutually exclusive in various cancer contexts [48].

CIN as a therapeutic target

Similar to what we demonstrate here, work from other groups has shown that presence of CIN can promote acquisition of drug resistance and is a mechanism to evade oncogene addition [5, 46]. Our data additionally show that suppression of segregation errors in cancer contexts is achievable and that reduction of CIN can limit mechanisms of acquired drug resistance. Indeed, due to its role in regulation of chromosome segregation, Aurora B is a provocative drug target and its inhibition has recently been shown to be efficacious in limiting proliferation of TKI-resistant NSCLC cells [49]. Together these data propose that pathways that promote CIN may serve as valuable drug targets, alone, or as co-therapies to enhance or prolong response to targeted therapeutic approaches.

Acknowledgements

This work was supported by a Smith Family Award for Excellence in Biomedical Research and R00CA182731 to ALM.

Author Contributions

ALM conceived and devised the study. ALM and NMH designed the experiments. ALM, NMH, EAC, and CPH performed the experiments. ALM wrote the manuscript with input and approval from all authors.

Declaration of Interests

Authors declare no competing interests

References

1. Baker, D.J., Jin, F., Jeganathan, K.B., and van Deursen, J.M. (2009). Whole chromosome instability caused by Bub1 insufficiency drives tumorigenesis through tumor suppressor gene loss of heterozygosity. Cancer cell *16*, 475-486.
2. Weaver, B.A., Silk, A.D., Montagna, C., Verdier-Pinard, P., and Cleveland, D.W. (2007). Aneuploidy acts both oncogenically and as a tumor suppressor. Cancer cell *11*, 25-36.
3. Choi, C.M., Seo, K.W., Jang, S.J., Oh, Y.M., Shim, T.S., Kim, W.S., Lee, D.S., and Lee, S.D. (2009). Chromosomal instability is a risk factor for poor prognosis of adenocarcinoma of the lung: Fluorescence in situ hybridization analysis of paraffin-embedded tissue from Korean patients. Lung Cancer *64*, 66-70.
4. McClelland, S.E., Burrell, R.A., and Swanton, C. (2009). Chromosomal instability: a composite phenotype that influences sensitivity to chemotherapy. Cell Cycle *8*, 3262-3266.
5. Sotillo, R., Schvartzman, J.M., Socci, N.D., and Benezra, R. (2010). Mad2-induced chromosome instability leads to lung tumour relapse after oncogene withdrawal. Nature *464*, 436-440.
6. Bakhoum, S.F., Genovese, G., and Compton, D.A. (2009). Deviant kinetochore microtubule dynamics underlie chromosomal instability. Curr Biol *19*, 1937-1942.
7. Godek, K.M., Kabeche, L., and Compton, D.A. (2015). Regulation of kinetochore-microtubule attachments through homeostatic control during mitosis. Nat Rev Mol Cell Biol *16*, 57-64.
8. Taylor, A.M., Shih, J., Ha, G., Gao, G.F., Zhang, X., Berger, A.C., Schumacher, S.E., Wang, C., Hu, H., Liu, J., et al. (2018). Genomic and Functional Approaches to Understanding Cancer Aneuploidy. Cancer Cell *33*, 676-689.e673.
9. Nagy, Á., Lánczky, A., Menyhárt, O., and Győrffy, B. (2018). Validation of miRNA prognostic power in hepatocellular carcinoma using expression data of independent datasets. Sci Rep *8*, 9227.
10. Hindriksen, S., Lens, S.M.A., and Hadders, M.A. (2017). The Ins and Outs of Aurora B Inner Centromere Localization. Front Cell Dev Biol *5*, 112.
11. González-Loyola, A., Fernández-Miranda, G., Trakala, M., Partida, D., Samejima, K., Ogawa, H., Cañamero, M., de Martino, A., Martínez-Ramírez, Á., de Cárcer, G., et al.

(2015). Aurora B Overexpression Causes Aneuploidy and p21Cip1 Repression during Tumor Development. Mol Cell Biol *35*, 3566-3578.

12. Abe, Y., Sako, K., Takagaki, K., Hirayama, Y., Uchida, K.S., Herman, J.A., DeLuca, J.G., and Hirota, T. (2016). HP1-Assisted Aurora B Kinase Activity Prevents Chromosome Segregation Errors. Dev Cell *36*, 487-497.
13. Broad, A.J., DeLuca, K.F., and DeLuca, J.G. (2020). Aurora B kinase is recruited to multiple discrete kinetochore and centromere regions in human cells. J Cell Biol *219*.
14. Hauf, S., Cole, R.W., LaTerra, S., Zimmer, C., Schnapp, G., Walter, R., Heckel, A., van Meel, J., Rieder, C.L., and Peters, J.M. (2003). The small molecule Hesperadin reveals a role for Aurora B in correcting kinetochore-microtubule attachment and in maintaining the spindle assembly checkpoint. J Cell Biol *161*, 281-294.
15. Muñoz-Barrera, M., and Monje-Casas, F. (2014). Increased Aurora B activity causes continuous disruption of kinetochore-microtubule attachments and spindle instability. Proc Natl Acad Sci U S A *111*, E3996-4005.
16. Huang, H., Lampson, M., Efimov, A., and Yen, T.J. (2018). Chromosome instability in tumor cells due to defects in Aurora B mediated error correction at kinetochores. Cell Cycle *17*, 2622-2636.
17. Kleyman, M., Kabeche, L., and Compton, D.A. (2014). STAG2 promotes error correction in mitosis by regulating kinetochore-microtubule attachments. J Cell Sci *127*, 4225-4233.
18. Manning, A.L., Benes, C., and Dyson, N.J. (2014). Whole chromosome instability resulting from the synergistic effects of pRB and p53 inactivation. Oncogene *33*, 2487-2494.
19. Manning, A.L., Yazinski, S.A., Nicolay, B., Bryll, A., Zou, L., and Dyson, N.J. (2014). Suppression of genome instability in pRB-deficient cells by enhancement of chromosome cohesion. Mol Cell *53*, 993-1004.
20. Barber, T.D., McManus, K., Yuen, K.W., Reis, M., Parmigiani, G., Shen, D., Barrett, I., Nouhi, Y., Spencer, F., Markowitz, S., et al. (2008). Chromatid cohesion defects may underlie chromosome instability in human colorectal cancers. Proc Natl Acad Sci U S A *105*, 3443-3448.
21. Sherwood, R., Takahashi, T.S., and Jallepalli, P.V. (2010). Sister acts: coordinating DNA replication and cohesion establishment. Genes Dev *24*, 2723-2731.
22. Kueng, S., Hegemann, B., Peters, B.H., Lipp, J.J., Schleiffer, A., Mechtler, K., and Peters, J.M. (2006). Wapl controls the dynamic association of cohesin with chromatin. Cell *127*, 955-967.
23. Yu, J., Zhou, J., Xu, F., Bai, W., and Zhang, W. (2018). High expression of Aurora-B is correlated with poor prognosis and drug resistance in non-small cell lung cancer. Int J Biol Markers *33*, 215-221.
24. Vischioni, B., Oudejans, J.J., Vos, W., Rodriguez, J.A., and Giaccone, G. (2006). Frequent overexpression of aurora B kinase, a novel drug target, in non-small cell lung carcinoma patients. Mol Cancer Ther *5*, 2905-2913.
25. Takeshita, M., Koga, T., Takayama, K., Ijichi, K., Yano, T., Maehara, Y., Nakanishi, Y., and Sueishi, K. (2013). Aurora-B overexpression is correlated with aneuploidy and poor prognosis in non-small cell lung cancer. Lung Cancer *80*, 85-90.

26. Ladurner, R., Kreidl, E., Ivanov, M.P., Ekker, H., Idarraga-Amado, M.H., Busslinger, G.A., Wutz, G., Cisneros, D.A., and Peters, J.M. (2016). Sororin actively maintains sister chromatid cohesion. EMBO J *35*, 635-653.
27. Nishiyama, T., Ladurner, R., Schmitz, J., Kreidl, E., Schleiffer, A., Bhaskara, V., Bando, M., Shirahige, K., Hyman, A.A., Mechtler, K., et al. (2010). Sororin mediates sister chromatid cohesion by antagonizing Wapl. Cell *143*, 737-749.
28. Masumoto, H., Masukata, H., Muro, Y., Nozaki, N., and Okazaki, T. (1989). A human centromere antigen (CENP-B) interacts with a short specific sequence in alphoid DNA, a human centromeric satellite. J Cell Biol *109*, 1963-1973.
29. Muro, Y., Masumoto, H., Yoda, K., Nozaki, N., Ohashi, M., and Okazaki, T. (1992). Centromere protein B assembles human centromeric alpha-satellite DNA at the 17-bp sequence, CENP-B box. J Cell Biol *116*, 585-596.
30. Pluta, A.F., Saitoh, N., Goldberg, I., and Earnshaw, W.C. (1992). Identification of a subdomain of CENP-B that is necessary and sufficient for localization to the human centromere. J Cell Biol *116*, 1081-1093.
31. Gazdar, A.F. (2009). Activating and resistance mutations of EGFR in non-small-cell lung cancer: role in clinical response to EGFR tyrosine kinase inhibitors. Oncogene *28 Suppl 1*, S24-31.
32. Gerber, D.E. (2008). EGFR Inhibition in the Treatment of Non-Small Cell Lung Cancer. Drug Dev Res *69*, 359-372.
33. Stewart, E.L., Tan, S.Z., Liu, G., and Tsao, M.S. (2015). Known and putative mechanisms of resistance to EGFR targeted therapies in NSCLC patients with EGFR mutations-a review. Transl Lung Cancer Res *4*, 67-81.
34. Arao, T., Fukumoto, H., Takeda, M., Tamura, T., Saijo, N., and Nishio, K. (2004). Small in-frame deletion in the epidermal growth factor receptor as a target for ZD6474. Cancer Res *64*, 9101-9104.
35. Vargas-Rondón, N., Villegas, V.E., and Rondón-Lagos, M. (2017). The Role of Chromosomal Instability in Cancer and Therapeutic Responses. Cancers (Basel) *10*.
36. Bakhoum, S.F., and Compton, D.A. (2012). Chromosomal instability and cancer: a complex relationship with therapeutic potential. J Clin Invest *122*, 1138-1143.
37. Chunduri, N.K., and Storchová, Z. (2019). The diverse consequences of aneuploidy. Nat Cell Biol *21*, 54-62.
38. Engelman, J.A., Zejnullahu, K., Mitsudomi, T., Song, Y., Hyland, C., Park, J.O., Lindeman, N., Gale, C.M., Zhao, X., Christensen, J., et al. (2007). MET amplification leads to gefitinib resistance in lung cancer by activating ERBB3 signaling. Science *316*, 1039-1043.
39. Tulchinsky, E., Demidov, O., Kriajevska, M., Barlev, N.A., and Imyanitov, E. (2019). EMT: A mechanism for escape from EGFR-targeted therapy in lung cancer. Biochim Biophys Acta Rev Cancer *1871*, 29-39.
40. Yochum, Z.A., Cades, J., Wang, H., Chatterjee, S., Simons, B.W., O'Brien, J.P., Khetarpal, S.K., Lemtiri-Chlieh, G., Myers, K.V., Huang, E.H., et al. (2019). Targeting the EMT transcription factor TWIST1 overcomes resistance to EGFR inhibitors in EGFR-mutant non-small-cell lung cancer. Oncogene *38*, 656-670.
41. Zhu, X., Chen, L., Liu, L., and Niu, X. (2019). EMT-Mediated Acquired EGFR-TKI Resistance in NSCLC: Mechanisms and Strategies. Front Oncol *9*, 1044.

42. Redmond, K.L., Papafili, A., Lawler, M., and Van Schaeybroeck, S. (2015). Overcoming Resistance to Targeted Therapies in Cancer. Semin Oncol *42*, 896-908.
43. Rajagopalan, H., and Lengauer, C. (2004). Aneuploidy and cancer. Nature *432*, 338-341.
44. Gao, C., Furge, K., Koeman, J., Dykema, K., Su, Y., Cutler, M.L., Werts, A., Haak, P., and Vande Woude, G.F. (2007). Chromosome instability, chromosome transcriptome, and clonal evolution of tumor cell populations. Proc Natl Acad Sci U S A *104*, 8995-9000.
45. Andersson, D.I., Slechta, E.S., and Roth, J.R. (1998). Evidence that gene amplification underlies adaptive mutability of the bacterial lac operon. Science *282*, 1133-1135.
46. Salgueiro, L., Buccitelli, C., Rowald, K., Somogyi, K., Kandala, S., Korbel, J.O., and Sotillo, R. (2020). Acquisition of chromosome instability is a mechanism to evade oncogene addiction. EMBO Mol Med *12*, e10941.
47. Orr, B., Talje, L., Liu, Z., Kwok, B.H., and Compton, D.A. (2016). Adaptive Resistance to an Inhibitor of Chromosomal Instability in Human Cancer Cells. Cell Rep *17*, 1755-1763.
48. Lengauer, C., Kinzler, K.W., and Vogelstein, B. (1998). Genetic instabilities in human cancers. Nature *396*, 643-649.
49. Bertran-Alamillo, J., Cattan, V., Schoumacher, M., Codony-Servat, J., Giménez-Capitán, A., Cantero, F., Burbridge, M., Rodríguez, S., Teixidó, C., Roman, R., et al. (2019). AURKB as a target in non-small cell lung cancer with acquired resistance to anti-EGFR therapy. Nat Commun *10*, 1812.

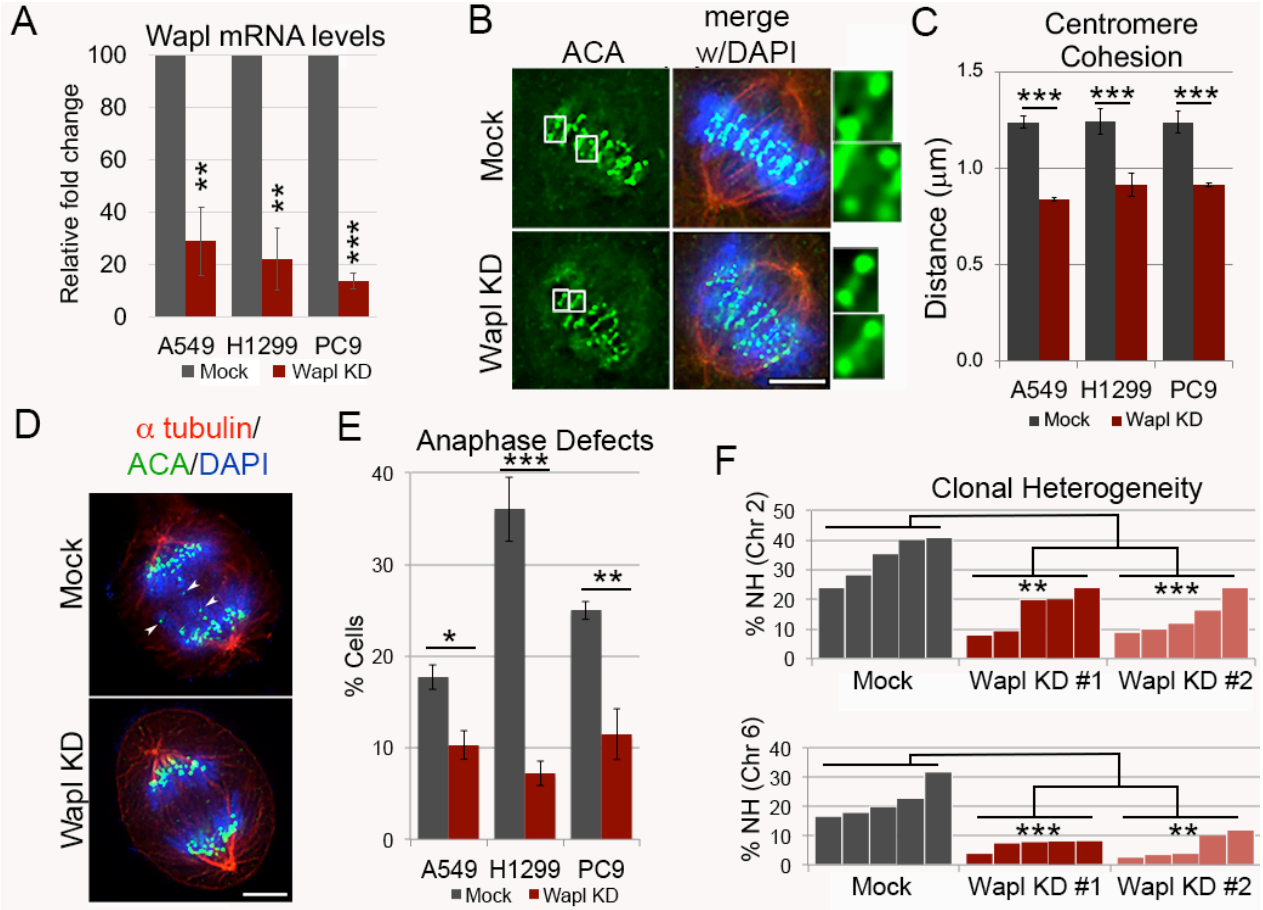

Figure 1: Wapl depletion suppresses CIN in NSCLC cells A) qPCR analysis of Wapl levels in control (Mock) and Wapl-depleted (Wapl KD) NSCLC cells. B & C) Representation and quantification of inter-centromere distances in PC9 cells with and without Wapl depletion. A minimum of 90 kinetochore pairs were measured (3/cell for 30 cells), for each of 3 biological replicates. Insets are of individual kinetochore pairs at 4x magnification. Scale bar is 5μm. D & E) Representation and quantification of anaphase lagging chromosomes in NSCLC cells with and without Wapl depletion. White arrow heads indicate individual lagging chromosomes in a PC9 anaphase cell. A minimum of 30 anaphase cells were scored per population for each of 3 biological replicates. F) Quantification of chromosome copy number heterogeneity (NH) in clonal populations of PC9 cells carrying an empty expression vector (pLKO.1) or one of two different shRNA constructs targeting Wapl for depletion (Wapl KD #1 and #2). Chromosome copy number was scored in a minimum of 300 cells for 5 clonal populations of each condition. Here and throughout *: p< 0.05, **: p<0.01; ***: p<0.001.

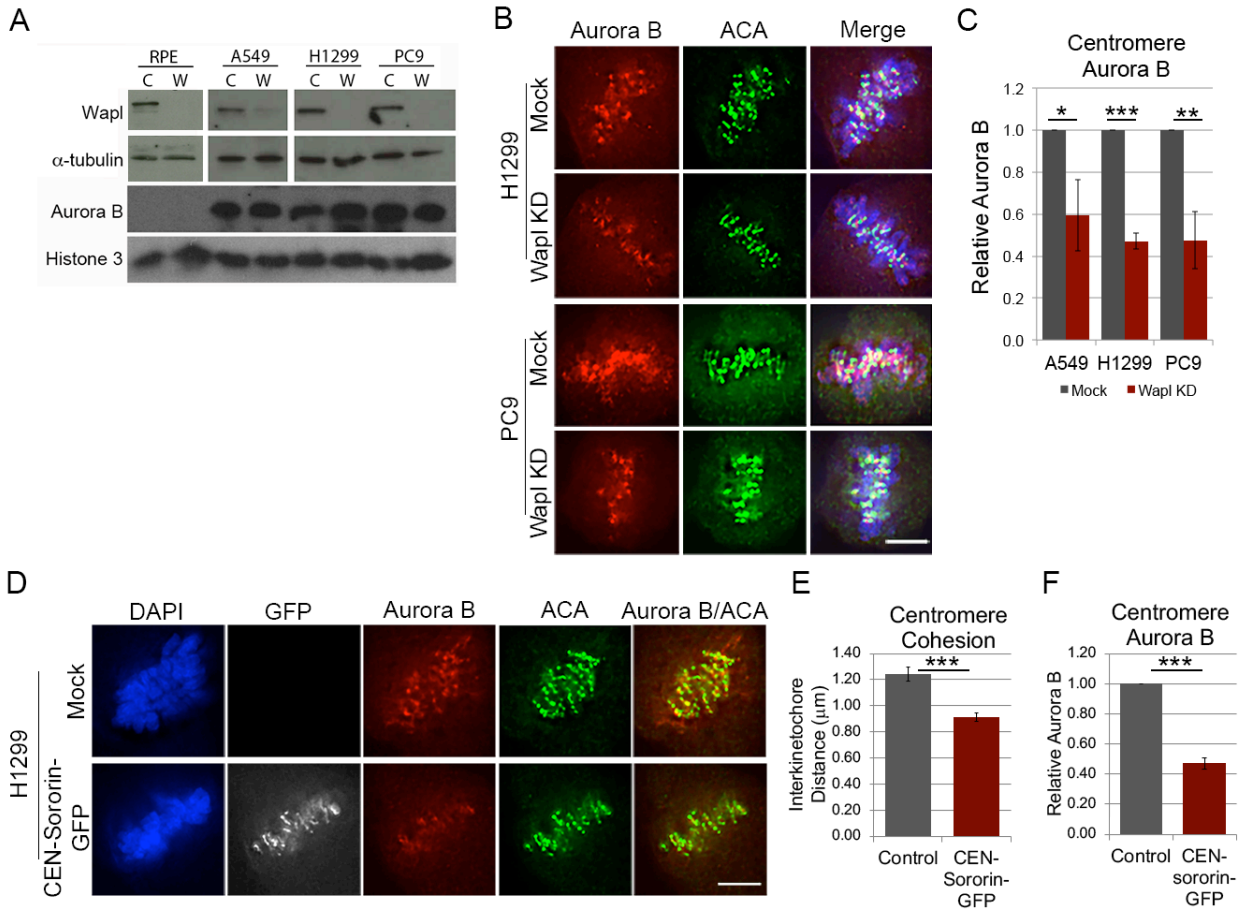

Figure 2: Aurora B in NSCLC cells is overexpressed and sensitive to centromere cohesion. A) Western blot analysis of Aurora B and Wapl levels in control (C) and Wapl-depleted (W) NSCLC cells. B & C) Representation and quantification of Aurora B levels at the centromere of NSCLC metaphase cells with (Wapl KD) and without (Mock) Wapl depletion. D-F) Representation and quantification of centromere cohesion and Aurora B levels at the centromere of control H1299 cells (Mock), and those expressing a centromere-targeted Sororin construct (CEN-Sororin-GFP). Scale bar is 5μm. A minimum of 90 kinetochore pairs were measured (3/cell for 30 cells), for each of 3 biological replicates. Scale bars are 5μm.

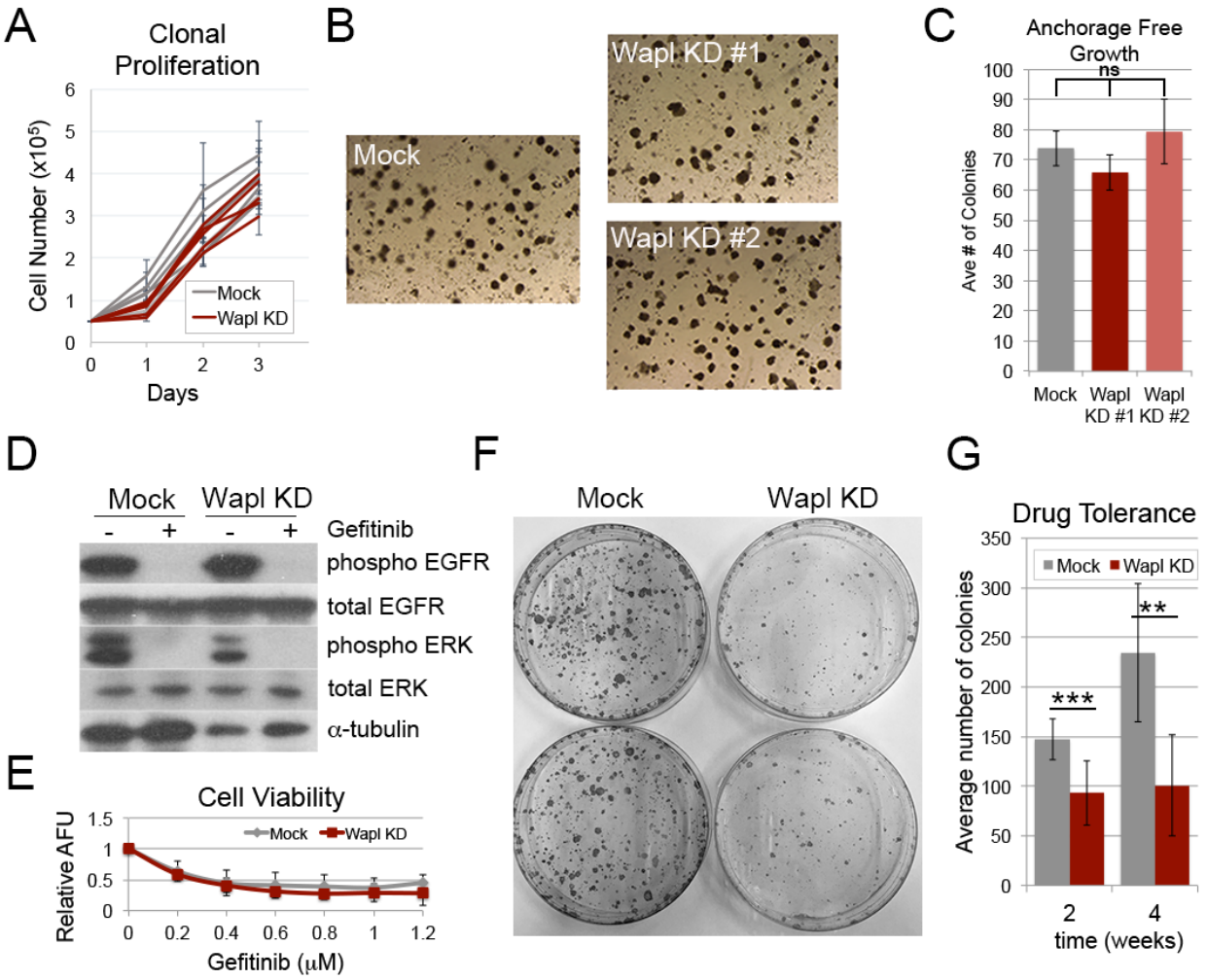

Figure 3. Suppression of CIN limits drug tolerance without compromising cell proliferation. A) Doubling times of 4 individual PC9 shWapl clones constitutively depleted of Wapl (Wapl KD) or not (Mock). B & C) Representation and quantification of average colony number formed by control (PLK0.1) and Wapl depleted (Wapl KD#1 & #2) cell lines cultured under anchorage-free conditions. D) Total and phosphorylated levels of EGFR and ERK in PC9 cells with mock and induced Wapl depletion following 2h exposure to 1μM Gefitinib. E) Cell viability following 3 days exposure to indicated concentrations of Gefitinib in mock and Wapl-depleted PC9 cells. F & G) Crystal Violet staining and quantification of emergent drug tolerant colony numbers following extended culture in media with 1μM Gefitinib. All experiments were performed in biological triplicate.

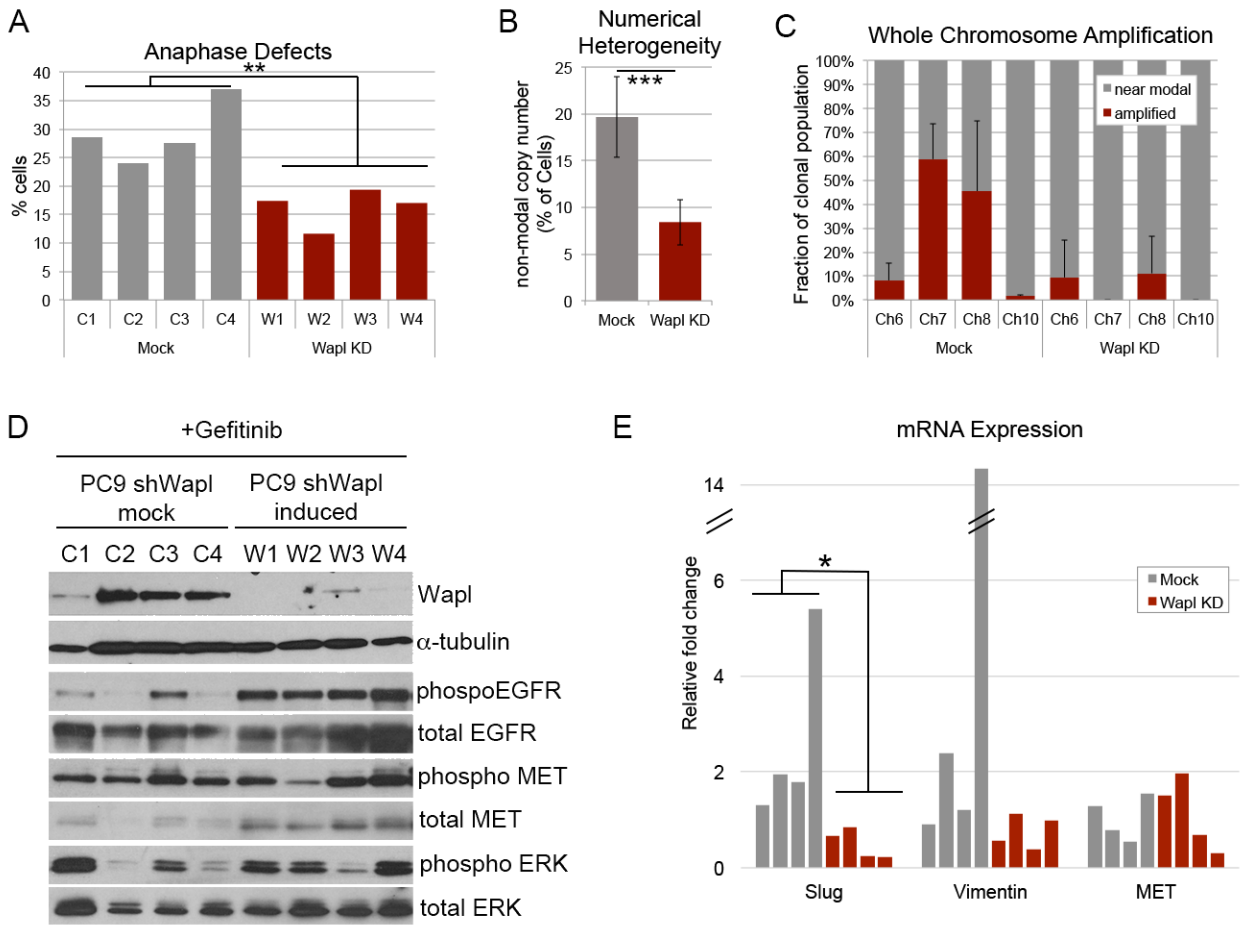

Figure 4: Suppression of CIN influences mechanisms of drug tolerance. A) Quantification of anaphase cells exhibiting lagging chromosomes in clonal populations of drug tolerant cells with (Wapl KD) or without (Mock) Wapl depletion. B & C) Gefitinib-tolerant PC9 cell clones derived with or without Wapl depletion labelled with centromere enumeration FISH probes for chromosomes 6, 7, 8, and 10 and quantified for intratumor numerical heterogeneity. D) Western blot showing Wapl levels and EGFR pathway status in four each of mock and Wapl-depleted drug tolerant clones. E) qPCR analysis of mRNA levels indicative of EMT pathway activation (slug, vimentin) and MET expression in mock and Wapl-depleted drug tolerant clones.

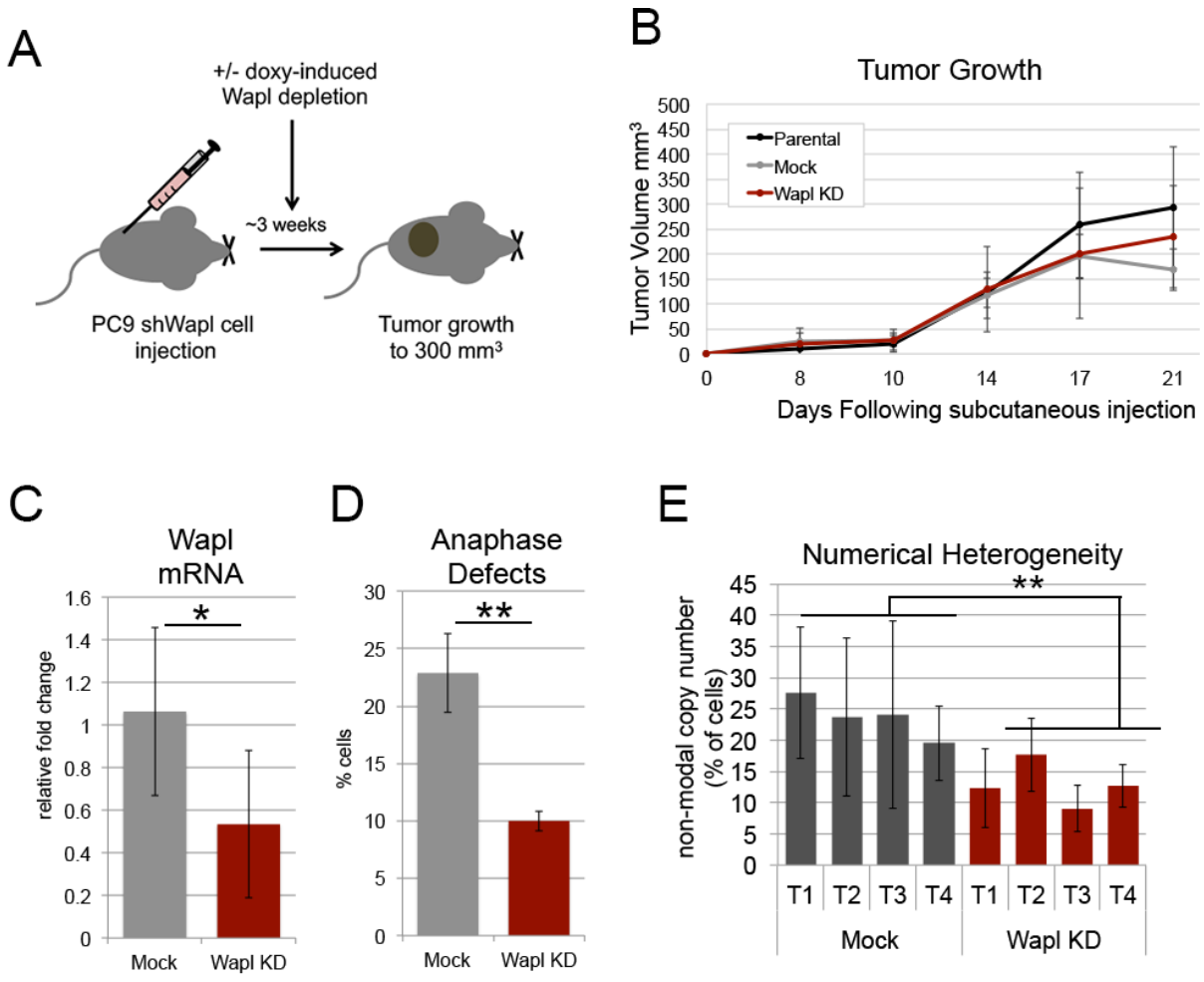

Figure 5. Wapl depletion is sufficient to suppress CIN *in vivo*. A) Diagram of experimental set up: PC9 cells carrying an inducible shWapl construct were injected into the flanks of mice. Doxycycline was administered in the drinking water of one cohort to induce Wapl depletion and tumor initiation and growth were monitored. B) Measures of tumor volume, through duration of initial growth of tumors with (Wapl KD) or without (Parental, Mock) depletion of Wapl. C) qPCR analysis of Wapl mRNA levels in tumors at 3 weeks of growth. D) Quantification of anaphase lagging chromosomes in cells derived from mock and shWapl-depleted tumors. Graphs in B-D reflect average values and standard deviations from 4 independent tumor populations per condition. E) Tumor cells labelled with centromere enumeration FISH probes for chromosomes 6, 7, 8, and 10 and quantified for intratumor numerical heterogeneity.

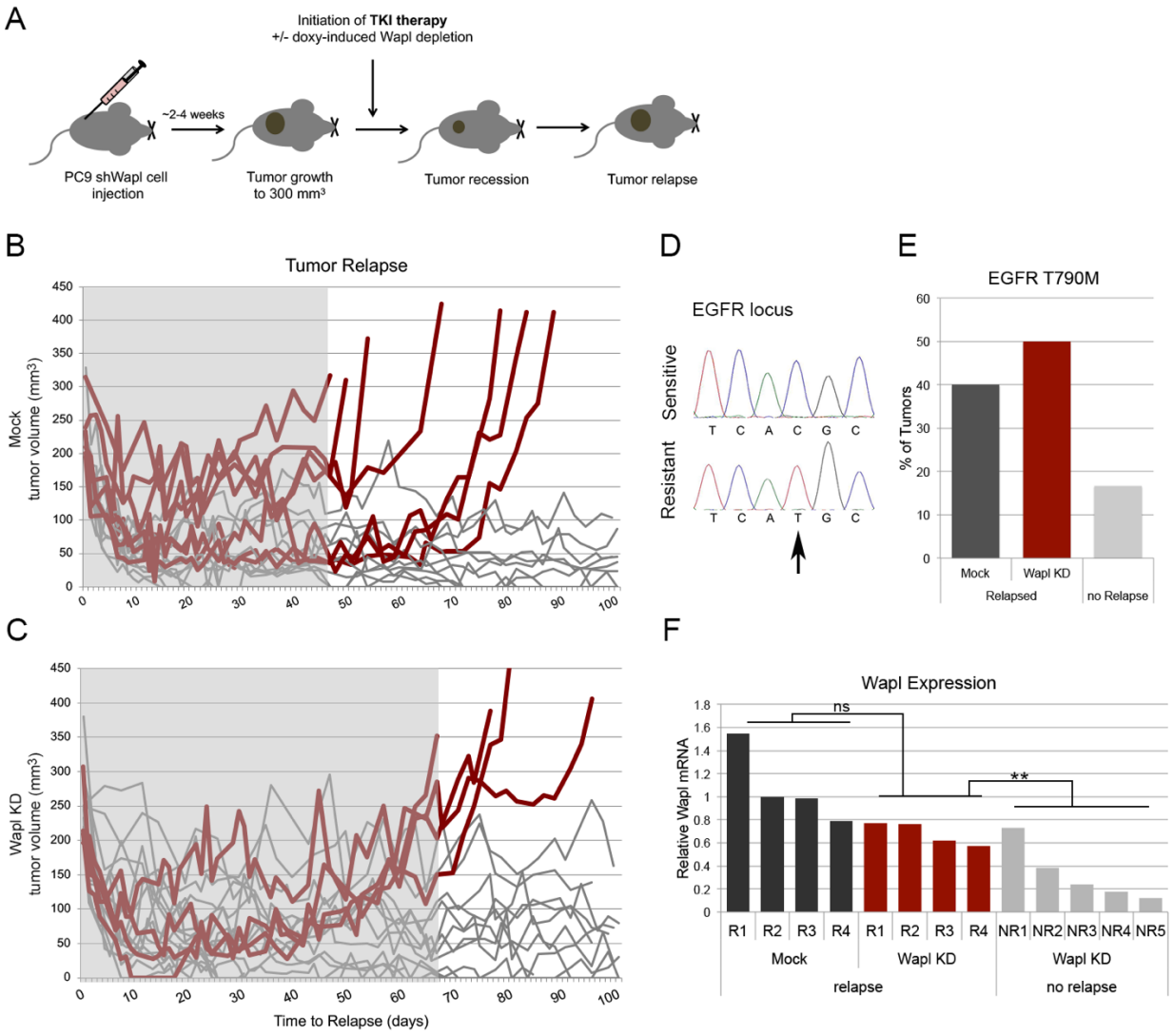

Figure 6. CIN is a driving force for acquired drug resistance. A) Diagram of experimental set up: PC9 cells carrying an inducible shWapl construct were injected into the flank of the mice. Once tumors reached 300mm^3 mice were split into two cohorts- one was administered doxycycline in drinking water to induce Wapl depletion concurrent with Gefitinib via oral gavage, the other received Gefitinib alone. All mice were monitored for initial tumor recession and relapse. B & C) Time to relapse of tumors with uninduced (n=19) and induced Wapl depletion (n= 19). Red lines indicate tumors that relapsed in this time frame, gray lines indicate those that remained responsive to treatment. Shaded box indicates the minimum relapse free response to Gefitinib in each cohort. D and E) Visualization and quantification of C → T mutation that results in the T790M mutation in EGFR that confers resistance to TKI. F) qPCR analysis of Wapl levels in control (Mock) and induced Wapl depletion (Wapl KD) that relapsed or not following Gefitinib treatment.

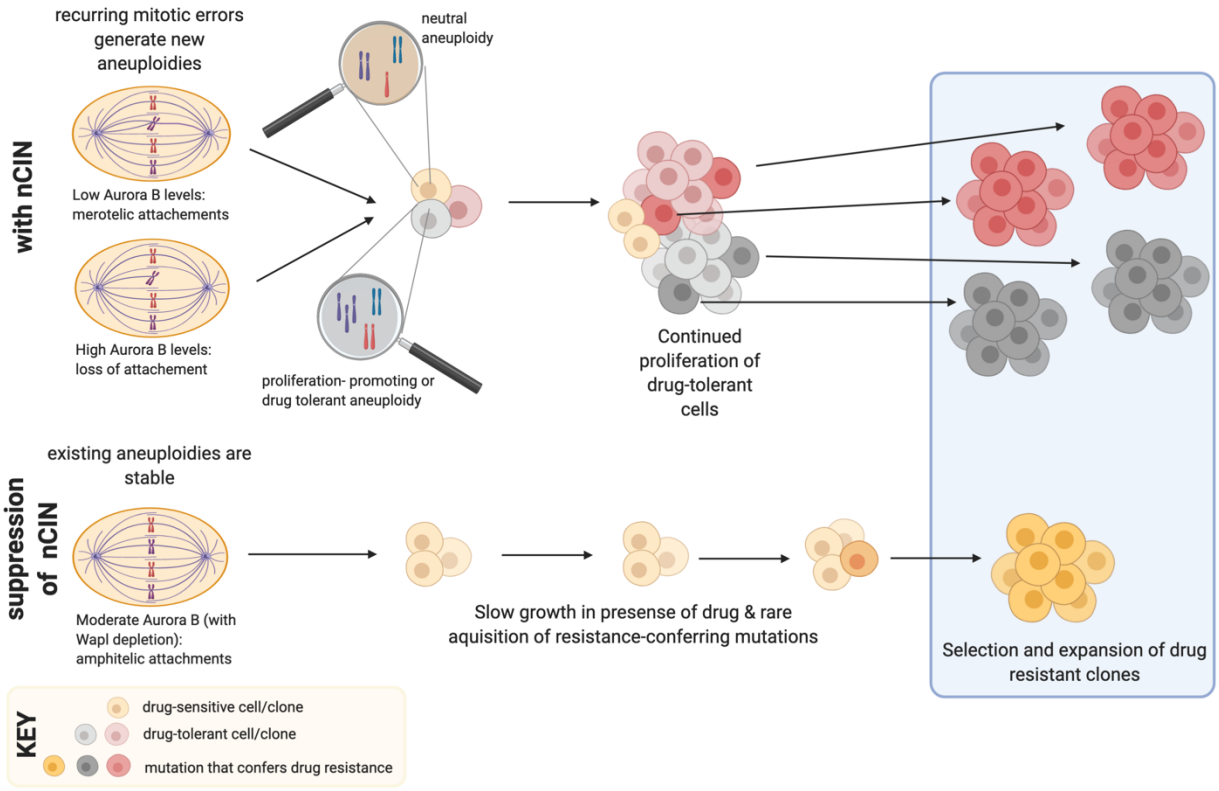

Figure 7: Mitotic defects that promote CIN enable generation of drug tolerant aneuploidies that permit continued growth and increased incidence of acquired drug resistance.